1521-0111/86/2/159–167$25.00
MOLECULAR PHARMACOLOGY

http://dx.doi.org/10.1124/mol.114.092338
Mol Pharmacol 86:159–167, August 2014

# Gating-Pore Currents Demonstrate Selective and Specific Modulation of Individual Sodium Channel Voltage-Sensors by Biological Toxins[S]

Yucheng Xiao, Kenneth Blumenthal, and Theodore R. Cummins

*Department of Pharmacology and Toxicology, Indiana University School of Medicine, Indianapolis, Indiana (Y.X., T.R.C.); Department of Biochemistry, School of Medicine and Biomedical Sciences, State University of New York, Buffalo, New York (K.B.)*

Received February 19, 2014; accepted June 4, 2014

**ABSTRACT**

Voltage-gated sodium channels are critical determinants of nerve and muscle excitability. Although numerous toxins and small molecules target sodium channels, identifying the mechanisms of action is challenging. Here we used gating-pore currents selectively generated in each of the voltage-sensors from the four α-subunit domains (DI–DIV) to monitor the activity of individual voltage-sensors and to investigate the molecular determinants of sodium channel pharmacology. The tarantula toxin huwentoxin-IV (HWTX-IV), which inhibits sodium channel current, exclusively enhanced inward gating-pore currents through the DII voltage-sensor. By contrast, the tarantula toxin ProTx-II, which also inhibits sodium channel currents, altered the gating-pore currents in multiple voltage-sensors in a complex manner. Thus, whereas HWTX-IV inhibits central-pore currents by selectively trapping the DII voltage-sensor in the resting configuration, ProTx-II seems to inhibit central-pore currents by differentially altering the configuration of multiple voltage-sensors. The sea anemone toxin anthopleurin B, which impairs open-channel inactivation, exclusively enhanced inward gating-pore currents through the DIV voltage-sensor. This indicates that trapping the DIV voltage-sensor in the resting configuration selectively impairs open-channel inactivation. Furthermore, these data indicate that although activation of all four voltage-sensors is not required for central-pore current generation, activation of the DII voltage-sensor is crucial. Overall, our data demonstrate that gating-pore currents can determine the mechanism of action for sodium channel gating modifiers with high precision. We propose this approach could be adapted to identify the molecular mechanisms of action for gating modifiers of various voltage-gated ion channels.

## Introduction

Voltage-gated sodium channels (VGSCs) are the primary generator of the upstroke of the action potential in electrically excitable cells, and abnormalities in VGSCs contribute to numerous inherited and acquired disorders of excitability (Waxman et al., 2000; George, 2005). A multitude of animal toxins target sodium channel voltage-sensors (Cestele and Catterall, 2000; Catterall, 2002; Blumenthal and Seibert, 2003). Many of these agents alter sodium current activity and channel gating with distinct voltage-dependent properties, suggesting that they differentially impact the voltage-sensors of VGSCs. However, it can be difficult to determine the precise mechanism of action of agents that target the gating activity of sodium channels.

VGSCs are complex transmembrane proteins composed of 24 transmembrane segments (Fig. 1A) arranged in four homologous α-subunit domains (DI–DIV), each having six transmembrane segments (S1–S6). The central pore of the channel is formed by the S5–S6 regions of each domain and the voltage-sensors by the S1–S4 regions. The highly charged S4 segments (Fig. 1B) in these complexes are surrounded by aqueous crevices that extend into the membrane from both the extracellular and intracellular surfaces. In the voltage-sensor a relatively short proteinaceous region separates the inner from the outer cavity. Normally ions do not traverse the voltage-sensor; rather, charged residues on the S4 segments (Arg or Lys) are transported from the inner crevice to the outer crevice during gating (Bezanilla, 2008). However, mutations of these charged S4 residues can induce "gating pores" and "gating-pore currents" (Starace and Bezanilla, 2004; Sokolov et al., 2005; Tombola et al., 2005; Struyk and Cannon, 2007; Tombola et al., 2007). Importantly, these gating-pore currents are ionic currents that do not flow through the central pore of the channel but rather flow through the modified VGSC voltage-sensors (Fig. 1C). The gating-pore currents generated by single-charge mutations and carried by cations such as $Na^+$ and $H^+$ are ≤1% of the central-pore current in VGSCs, but in potassium channels, because of their 4-fold symmetry, they can be larger (~6% of the central-pore current) (Sokolov et al., 2005). Depending on which charged residues in the S4 segments are

This work was supported by a grant from the National Institutes of Health National Institute of Neurological Disorders and Stroke [NS077805] (to T.R.C.)
dx.doi.org/10.1124/mol.114.092338.
[S] This article has supplemental material available at molpharm.aspetjournals.org.

**ABBREVIATIONS:** ApB, anthopleurin B; DI–DIV, α-subunit domains I–IV; HEK293, human embryonic kidney 293; HWTX-IV, huwentoxin-IV; Igp, gating-pore current; I–V, current-voltage; $Na_v$, voltage-gated sodium channel; TTX, tetrodotoxin; VGSCs, voltage-gated sodium channels; WT*, wild type*; WT, wild type.

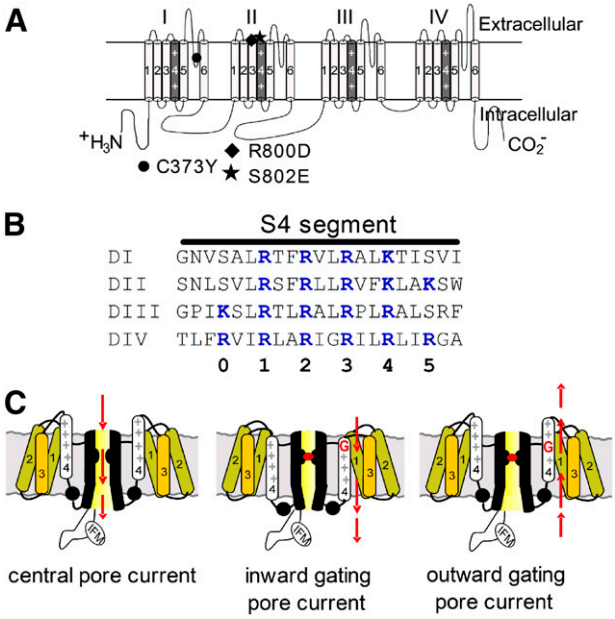


**Fig. 1.** Diagrams of voltage-gated sodium channels. (A) Schematic diagram of sodium channel $\alpha$-subunit $Na_v$ 1.5 (upper). The voltage-sensor (S4 segment) of each domain is shaded in gray and marked with "++". The $\alpha$-subunit contains three mutation sites: C373Y (filled circle), TTX-sensitive; R800D (filled diamond) and S802E (filled pentagon), HWTX-IV-sensitive. (B) Amino acid sequences of four S4 segments are aligned. The gating-charge residues (Lys/Arg) are highlighted in blue and the numbering scheme for these residues is shown below. (C) Schematic diagram depicting channel central-pore current (left panel), inward gating-pore current with central-pore current blocked (middle panel), and outward gating-pore current with central-pore current blocked (right panel).

mutated, gating-pore currents arise either in the resting or the activated configuration (Sokolov et al., 2007; Sokolov et al., 2008b) (Fig. 1C). Monitoring gating-pore currents can provide unique insight into the configuration of individual voltage-sensors and how they respond to changes in transmembrane voltage.

We mutated the outer charged residues to induce inward gating-pore currents in the resting configuration. We show that inward gating-pore currents generated by each of the individual voltage-sensors can be measured from channels expressed in a mammalian cell line. We demonstrate that gating-pore currents can be used to precisely identify and monitor the ability of toxins to modulate the activity of the individual voltage-sensors.

## Materials and Methods

**Toxins.** Anthopleurin B (ApB) was recombinantly produced as described by Gallagher and Blumenthal (1992). ProTx-II and huwentoxin-IV (HWTX-IV) were chemically synthesized as described by Middleton et al. (2002) and Xiao et al. (2008), respectively.

**Plasmids and Construction of Sodium Channel Mutants.** The cDNA genes encoding the tetrodotoxin- (TTX) and HWTX-IV-sensitive $Na_v$ 1.5 (C373Y/R800D/S802E) and auxiliary subunit $\beta$1 were cloned from human and subcloned into the pcDNA3.1 vector ($Na_v$ 1.5) and an internal ribosome entry site vector ($\beta$1) (Lossin et al., 2002). All mutations inserted into the sodium channel cDNA gene were constructed using the QuickChange II XL Site-Directed Mutagenesis kit (Agilent Technologies, Santa Clara, CA) according to the manufacturer's instruction. All constructs were sequenced to confirm that the appropriate mutations were made. The TTX- and HWTX-IV-sensitive modified wild-type $Na_v$ 1.5 channel is referred to as wild type* (WT*) in this study.

**Transient Transfection.** Transient transfection of $hNa_v$ 1.5 constructs into human embryonic kidney 293 (HEK293) cells was performed using the calcium phosphate precipitation method. HEK293 cells were grown under standard tissue culture conditions (5% $CO_2$ and 37°C) in Dulbecco's modified Eagle's medium supplemented with 10% fetal bovine serum (FBS). All $hNa_v$ 1.5 mutant channels were cotransfected with the h$\beta$1-subunit to increase current density. The calcium phosphate-DNA mixture (channel constructs and a green fluorescent protein reporter plasmid) was added to the cell culture medium and left for 3–4 hours, after which the cells were washed with fresh medium. Cells with green fluorescent protein fluorescence were selected for whole-cell patch-clamp recordings 36–72 hours after transfection.

**Electrophysiological Recordings.** Ionic currents were recorded at room temperature (~21°C) using an EPC-10 amplifier and the PulseFit program (Version 8.31; HEKA, Lambrecht/Pfalz, Germany). Fire-polished electrodes were fabricated from 1.7-mm capillary glass (VWR, West Chester, PA) using a P-97 puller (Sutter Instrument Company, Novato, CA). To minimize capacitive artifacts, the electrode tips were coated with sticky wax (Coltène/Whaledent Inc., Cuyahoga Falls, OH). After filling with the intracellular solution containing (in mM): CsF 140, EGTA 1.1, NaCl 10, and HEPES 10, pH 7.3 (adjusted with HCl), the access resistance of electrode pipettes ranged between 0.9 and 1.8 MΩ. The intracellular solution for recording outward gating-pore current contained (in mM): CsF 130, guanidine sulfate 10 mM, EGTA 1.1, NaCl 10, and HEPES 10, pH 7.3 (adjusted with HCl). The bathing solution was (in mM): NaCl 140, $MgCl_2$ 1, $CaCl_2$ 3, and HEPES 10, pH 7.3 (adjusted with NaOH). The liquid junction potential for these solutions was <8 mV; data were not corrected to account for this offset. The offset potential was zeroed before patching. After establishing the whole-cell recording configuration, the cells were held at −100 mV for 5 minutes. A P/–5 subtraction protocol was used to remove linear leak current and capacitance artifact only for data shown in Figs. 4, A and B, and 6, A and B; no online subtraction was performed in other experiments. Ion currents were filtered at 5 kHz and sampled at 20 kHz. Voltage errors were minimized using 70–80% series resistance compensation.

Toxin stock solutions were made at 100 $\mu$M using the bathing solution containing 1 mg/ml bovine serum albumin, and aliquots were stored at −20°C. Before use, the solution was diluted to the concentrations of interest with fresh bathing solution. Toxin was diluted into the recording chamber (volume of 300 $\mu$l) and mixed by repeatedly pipetting 30 $\mu$l to achieve the specified final concentration.

**Data Analysis.** Data were analyzed using the software programs PulseFit (HEKA) and GraphPad Prism 5.0 (GraphPad Software, Inc., San Diego, CA). All data are shown as mean ± S.E. The number of separate experimental cells is presented as $n$. The "activation threshold" for gating-pore currents (see Figs. 2, 3, 5, and 7) was defined as the most positive voltage at which gating-pore current can be observed above the baseline noise measured at fully depolarized potentials (i.e., 0 mV), and was judged by eye. Statistical analysis was carried out by Student's $t$ test, and $P < 0.05$ indicated a significant difference.

## Results

**Quantification of Sodium Channel Gating-Pore Currents in Mammalian Cells.** Our goal was to determine if gating-pore currents could be used to investigate the mechanisms of interaction for toxins that modify VGSCs. Although gating-pore currents have been observed in *Xenopus* oocytes, they have not previously been recorded from mammalian heterologous expression systems such as HEK293 cells. We used

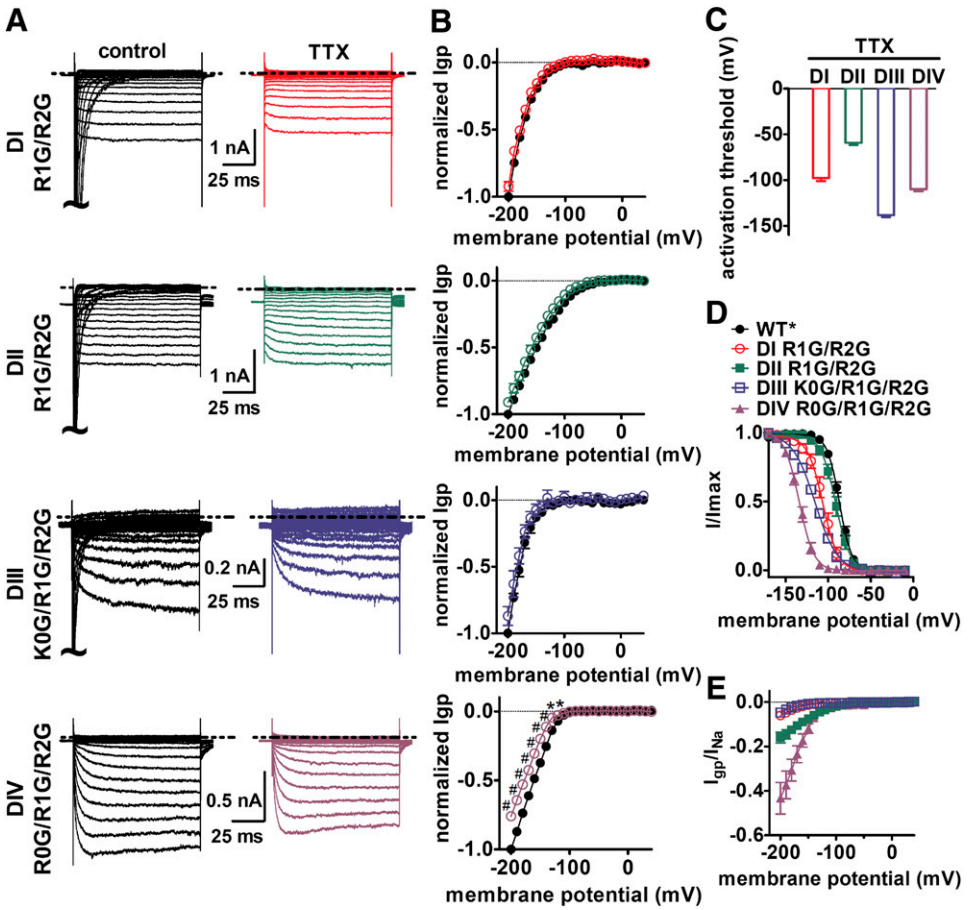


**Fig. 2.** Inward gating-pore current (Igp) were generated by mutations of the charged residues in the individual DI–DIV voltage-sensors of $Na_v$ 1.5. (A) Typical current traces before (left) and after (right) 1 $\mu$M TTX treatment were elicited by 100-ms hyperpolarizing steps to various potentials that ranged from –200 to +40 mV in a 10-mV increment. The cells were held at –100 mV. The dotted line represents the zero current level. Linear leak and capacitance currents were not subtracted. (B) Effects of TTX on the current-voltage (I–V) curves of inward Igp. The subtraction of linear leak currents has been performed in the absence (filled circles) or presence (open circles) of 1 $\mu$M TTX. Igp were normalized to the maximal control Igp. (C) Activation threshold of Igp through the four voltage-sensors measured in the presence of TTX. (D) Effects of Gly mutations of gating-charge residues in four S4 segments on steady-state inactivation. The voltage dependence of steady-state inactivation was estimated using a standard double-pulse protocol. Currents were plotted as a fraction of the maximal peak current. Data points were fitted with a standard Boltzmann equation. (E) Ratio of Igp to the total central-pore current ($I_{Na}$). $I_{Na}$ was estimated by the equation: $I_{Na} = I_{-100}/hinf_{-100}$, in which $I_{-100}$ is the maximal central-pore current when cells were held at –100 mV, and $hinf_{-100}$ is the fraction of the total sodium channels available at –100 mV on the basis of steady-state inactivation curve as shown in (D). $^{*}P < 0.05$; $^{\#}P < 0.01$.

HEK293 cells here because voltage-gated ion channels may be have a greater tendency to undergo normal posttranslational modifications in mammalian cells than in *Xenopus* oocytes, which could be an advantage in dissecting toxin-channel interactions.

We first determined if we could obtain measureable gating-pore currents from each of the four individual voltage-sensors for a VGSC expressed in a mammalian cell line. To maximize our chances for success, we chose to use human $Na_v$ 1.5 VGSCs, which routinely generate large central-pore currents (often up to 50 nA) compared with other VGSCs. For our studies we used a $hNa_v$ 1.5 construct that was modified to be sensitive to the pore blocker TTX (Satin et al., 1992) and the gating modifier HWTX-IV (Xiao et al., 2008). Hereafter this $hNa_v$ 1.5-C373Y/R800D/S802E construct will be referred to as WT* to distinguish it from the subsequent gating-pore constructs containing additional mutations. In the WT* construct, 1 $\mu$M TTX blocked virtually all of the transient sodium current conducted by the central pore (Supplemental Fig. 1A). In the presence of TTX, cells expressing WT* channels exhibited only linear leak currents; no gating-pore currents were observed (Supplemental Fig. 1B). To obtain measureable gating-pore currents from each of the individual voltage-sensors, we made a series of single, double, and triple mutations in each domain where charged residues in the S4 segment (Fig. 1B) were mutated to glycine residues. Although we were unable to reliably measure gating-pore currents in HEK293 cells from channels with single mutations, mutating the first and second arginines in DI and DII to glycine (R1G/R2G) yielded resolvable gating-pore currents at negative membrane potentials (Fig. 2A). To obtain measureable gating-pore currents from DIII and DIV, we found it necessary to mutate three charged residues in the S4 segments (K0G/R1G/R2G and R0G/R1G/R2G for DIII and DIV, respectively). For each of these constructs, the peak transient central-pore current was blocked by the addition of TTX (Fig. 2A, right panels). As was recently reported with $Na_v$ 1.4 gating-pore currents measured in *Xenopus* oocytes (Capes et al., 2012), TTX failed to alter the gating-pore currents in the voltage-sensor subdomains of DI, DII, and DIII, but slightly reduced the gating-pore current amplitude of DIV ($P < 0.05$; Fig. 2B). This is consistent with the notion that TTX can subtly impact the configuration of the DIV voltage-sensor. By contrast, the gating-pore currents generated in each of the four voltage-sensors were substantially inhibited by 1 mM gadolinium (Supplemental Fig. 2), consistent with previous studies in *Xenopus* oocytes (Sokolov et al., 2010). Interestingly, the voltage dependence of steady-state inactivation was altered by charge mutations in DI, DIII, and DIV, but not DII (Fig. 2D). The amplitude of the gating-pore currents, relative to the peak transient central-pore current generated by the different domains, also differed significantly for the four voltage-sensors, with DII and DIV mutations generating the largest relative gating-pore currents (Fig. 2E).

**Gating-Pore Current Analysis Demonstrates that HWTX-IV Selectively Traps DII in the Resting Position.** We next asked if gating-pore currents could be used to characterize toxin-channel interactions. Previously we have

used extensive site-directed mutagenesis to show that tarantula toxin HWTX-IV inhibition of central-pore currents critically depends on specific residues in the DII voltage-sensor (Xiao et al., 2008; Xiao et al., 2011), suggesting that HWTX-IV indirectly inhibited central-pore currents by blocking movement of a voltage-sensor, and thus preventing activation of the channel. We examined the effects of HWTX-IV on inward gating-pore currents generated by each of the four voltage-sensors and found that HWTX-IV only significantly altered the gating-pore currents generated in DII (Fig. 3, A and B). HWTX-IV substantially enhanced the amplitude of the gating-pore currents in DII and shifted the activation threshold for these inward DII gating-pore currents by more than 50 mV in the depolarizing direction (Fig. 3C). The modulation of DII gating-pore currents by HWTX-IV was abolished by point mutations in the DII voltage-sensor (D800R/E802S) that also abolish the ability of HWTX-IV to inhibit the transient central-pore currents (Fig. 4) (Xiao et al., 2008). These data confirm that HWTX-IV specifically interacts with the DII voltage-sensor and provide compelling evidence that HWTX-IV inhibits central pore sodium currents by selectively trapping the DII voltage-sensor in the resting position, preventing channel activation.

**Gating-Pore Current Analysis Demonstrates that Anthopleurin B Selectively Traps DIV in the Resting Position.** We also examined the effect of the sea anemone toxin anthopleurin B (ApB) on the VGSC gating-pore currents. ApB substantially enhances VGSC currents by selectively impairing fast inactivation (Benzinger et al., 1998). We found that ApB significantly enhanced the gating-pore currents generated in DIV (Fig. 5, A and B), shifting the threshold for activation of the inward gating-pore currents by almost +80 mV (Fig. 5C), although having no effect on the gating-pore currents generated by DI, DII, and DIII. Because TTX also can impact DIV gating-pore currents, we measured the effect of a saturating concentration of ApB on DIV gating-pore currents in the absence and presence of TTX. The effects of ApB on DIV gating-pore currents were observed in the absence and presence of TTX (Supplemental Fig. 3), indicating that whereas TTX can still bind to sodium channels in the presence of ApB, the impact of ApB on DIV gating-pore currents dominates that of TTX. Site-directed mutagenesis previously identified an aspartate residue (corresponding to D1610 in $hNa_v$ 1.5) in the extracellular portion of the DIV voltage-sensor that was crucial to ApB's ability to disrupt fast inactivation (Benzinger et al., 1998). The effects on DIV gating-pore currents were abolished by the D1610R mutation that nearly eliminates the effect of ApB on sodium channel inactivation kinetics (Fig. 6). Thus ApB impairs sodium current inactivation by selectively trapping the DIV voltage-sensor in the resting position.

**ProTx-II Has Unique Interactions with Multiple Sodium Channel Voltage-Sensors.** We next examined the effect of the tarantula toxin ProTx-II on VGSC gating-pore

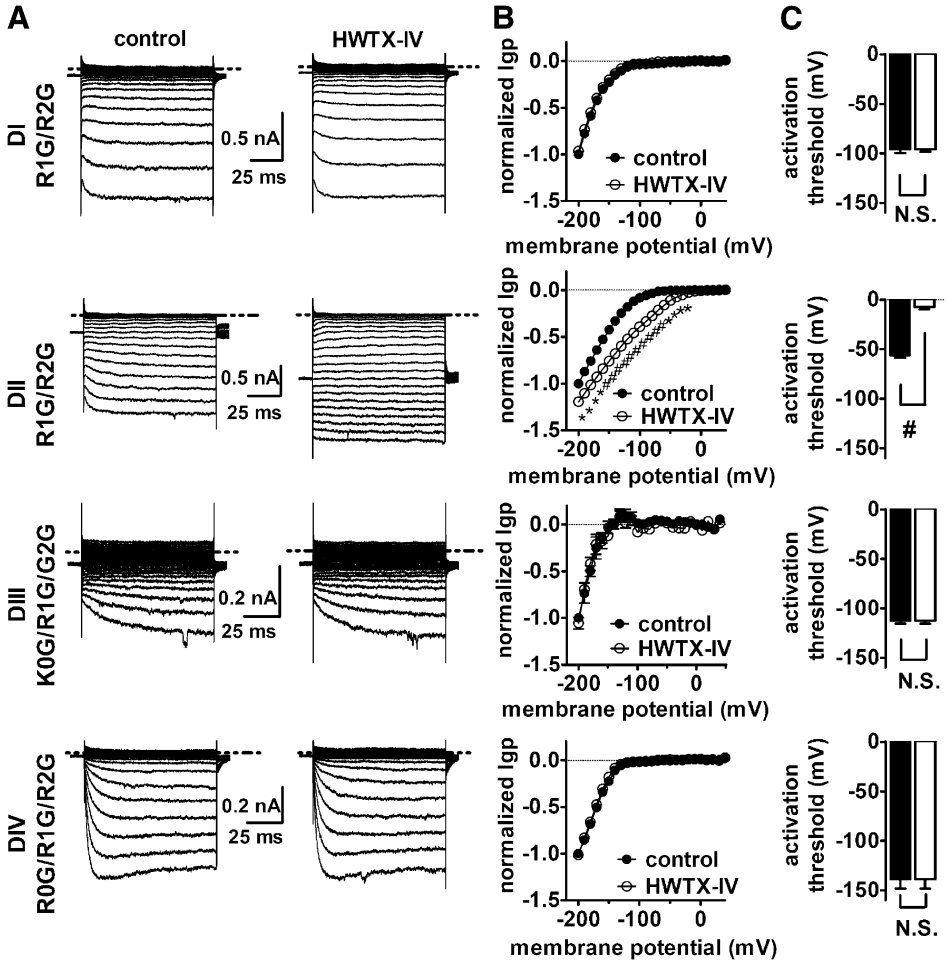


**Fig. 3.** Effect of HWTX-IV on inward Igp generated by DI–DIV voltage-sensor mutants. (A) Typical inward $hNa_v$ 1.5 Igp current traces before and after 1 $\mu$M HWTX-IV treatment. Cells were held at –100 mV and pretreated with 1 $\mu$M TTX. Currents before (left) and after (right) toxin treatment were elicited by 100-ms hyperpolarizing steps to various potentials that ranged from –200 mV to +40 mV in a 10-mV increment. The dotted line across current traces represents the zero current level. Linear leak and capacitance currents were not subtracted. (B) Effect of HWTX-IV on the I–V curves of inward Igp. In the I–V curves, the subtraction of linear leak currents has been performed before (filled circles) and after (open circles) application of 1 $\mu$M HWTX-IV. Igp were normalized to the maximal control Igp. (C) Effect of HWTX-IV on the activation threshold of Igp fluxing through four voltage-sensors, respectively. N. S., no significance; $^{*}P < 0.05$; $^{\#}P < 0.01$.

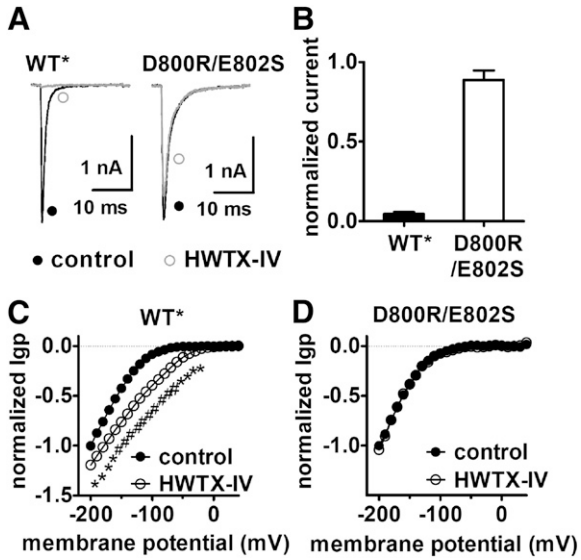


**Fig. 4.** The double mutation (D800R/E802S) abolished the ability of HWTX-IV to alter the inward Igp fluxing through DII voltage-sensor mutant. (A) Effects of HWTX-IV on the central-pore currents from the WT* and double mutant R800D/S802E $Na_v$ 1.5 channels. Current traces before (black) and after (gray) 1 $\mu$M HWTX-IV treatment were induced by a 20-ms depolarizing potential of –10 mV from a holding potential of –100 mV. (B) Fraction of remaining currents in the presence of 1 $\mu$M HWTX-IV. (C) HWTX-IV positively shifted the I–V curve of the inward Igp generated by $hNa_v$ 1.5 DII voltage-sensor mutant (R1G/R2G). (D) Double mutation D800R/E802S abolished the effect of HWTX-IV on the inward Igp generated by DII voltage-sensor mutant (R1G/R2G). In both (C) and (D) Igp were elicited by the protocol as described in the legend of Supplemental Fig. 3. Cells were held at –100 mV and pretreated with 1 $\mu$M TTX. All currents are normalized to the maximal control current amplitude. Linear leak currents were subtracted.

currents. Although several studies have investigated the effects of ProTx-II on VGSCs, the details of the interaction remain unclear. ProTx-II can inhibit the central-pore current of multiple VGSC isoforms (Middleton et al., 2002) but is most potent against $Na_v$ 1.7 (Schmalhofer et al., 2008). Several studies have used site-directed mutagenesis to identify specific residues in the DII voltage-sensor that can partially reduce the inhibitory action of ProTx-II (Schmalhofer et al., 2008; Sokolov et al., 2008a), suggesting that in part ProTx-II inhibition may be attributable to trapping of the DII voltage-sensor in the closed state. However, extensive analyses of sodium channel chimeras have been unable to confirm the role of the DII voltage-sensor as the sole determinant of ProTx-II inhibition of $Na_v$ 1.5, suggesting the toxin might interact with VGSCs in a novel manner (Smith et al., 2007). Paddle chimeras, where the S3–S4 linker of each VGSC domain was transplanted into a potassium channel, indicated that ProTx-II can interact with the voltage-sensors in DI, DII, and DIV (Bosmans et al., 2008). Previously, we reported that ProTx-II could both inhibit the peak transient pore current of $Na_v$ 1.7, in part by interacting with residues in the DII voltage-sensor, and impair inactivation of $Na_v$ 1.7 through interactions with residues in DIV (Xiao et al., 2010). Here we show that ProTx-II significantly alters the gating-pore currents generated by the DI, DII, and DIV voltage-sensors (Fig. 7). The impact on the DIV gating-pore currents was relatively minor but significant, which is consistent with our previous study indicating that the impairment of $hNa_v$ 1.5 inactivation by ProTx-II is ~50-fold less potent than the inhibitory effect on central-pore current activation. However, ProTx-II is ~15-fold more potent at impairing inactivation of $hNa_v$ 1.7 than $hNa_v$ 1.5 DIV (Xiao et al., 2010). Therefore, we asked if ProTx-II was able to inhibit $hNa_v$ 1.7 DIV gating-pore current to a greater extent than that of $hNa_v$ 1.5, and this was indeed what we observed (Supplemental Fig. 4).

ProTx-II had mixed effects on DII gating-pore currents, inhibiting them at extreme negative potentials ($< -180$ mV) but substantially enhancing them between –160 and –10 mV. Surprisingly, ProTx-II substantially inhibited the gating-pore currents through the DI voltage-sensor, suggesting that ProTx-II destabilizes the resting state of this voltage-sensor. To investigate this we created additional mutations in each of the $hNa_v$ 1.5 WT* voltage-sensors in an attempt to generate outward gating-pore currents that would flow at depolarized potentials when the voltage-sensors were at activated positions (see schematic diagram in Fig. 1C). We were unsuccessful in generating outward gating-pore currents through the DIII and DIV voltage-sensors but did obtain them in the DI and DII voltage-sensors after mutating the 3rd and 4th charged residues to glycine (Supplemental Fig. 5). These outward gating-pore currents were inhibited by 1 mM gadolinium (Supplemental Fig. 6). Both ProTx-II and HWTX-IV substantially blocked the outward gating-pore currents through the DII voltage-sensor (Fig. 8, C and D). This, in combination with the ability of both toxins to enhance inward gating-pore currents in DII, is consistent with the proposal that these toxins both trap the DII voltage-sensor in the resting configuration. ProTx-II also substantially blocked the outward gating-pore currents generated in DI (Fig. 8A), shifting the threshold for activation by +50 mV or more. Taken together, these data on ProTx-II effects on inward and outward gating-pore currents indicate that ProTx-II does not trap the DI voltage-sensor in either the resting or activated configuration, but rather locks it in an intermediate state, preventing it from reaching the fully activated configuration. However, because ProTx-II may interact with both the DII and DIV voltage-sensors, which flank the DI voltage-sensor, an alternative possibility was that ProTx-II only indirectly modifies the activity of the DI voltage-sensor. To test this possibility, we examined the effect of simultaneously applying both HWTX-IV and ApB on DI gating-pore currents. In contrast to ProTx-II, coapplication of HWTX-IV and ApB had only a minor inhibitory effect on the outward gating-pore currents in DI (Fig. 8B) and the inward gating-pore currents generated by the R1G/R2G mutations in DI (Supplemental Fig. 7). These data indicate that trapping both the DII and DIV voltage-sensors in the resting state has only a small impact on the movement of the DI voltage-sensor, and thus confirm that ProTx-II most probably blocks sodium channel activation by directly interacting with the DI as well as the DII voltage-sensor.

## Discussion

VGSCs are intimately involved in normal and abnormal electrical excitability in a multitude of tissues. Although numerous animal toxins and drugs can alter sodium currents and sodium channel gating, it is difficult to determine how specific agents alter the activity of individual sodium channel voltage-sensors. Here we used gating-pore currents to investigate the impact of three different peptide toxins on each

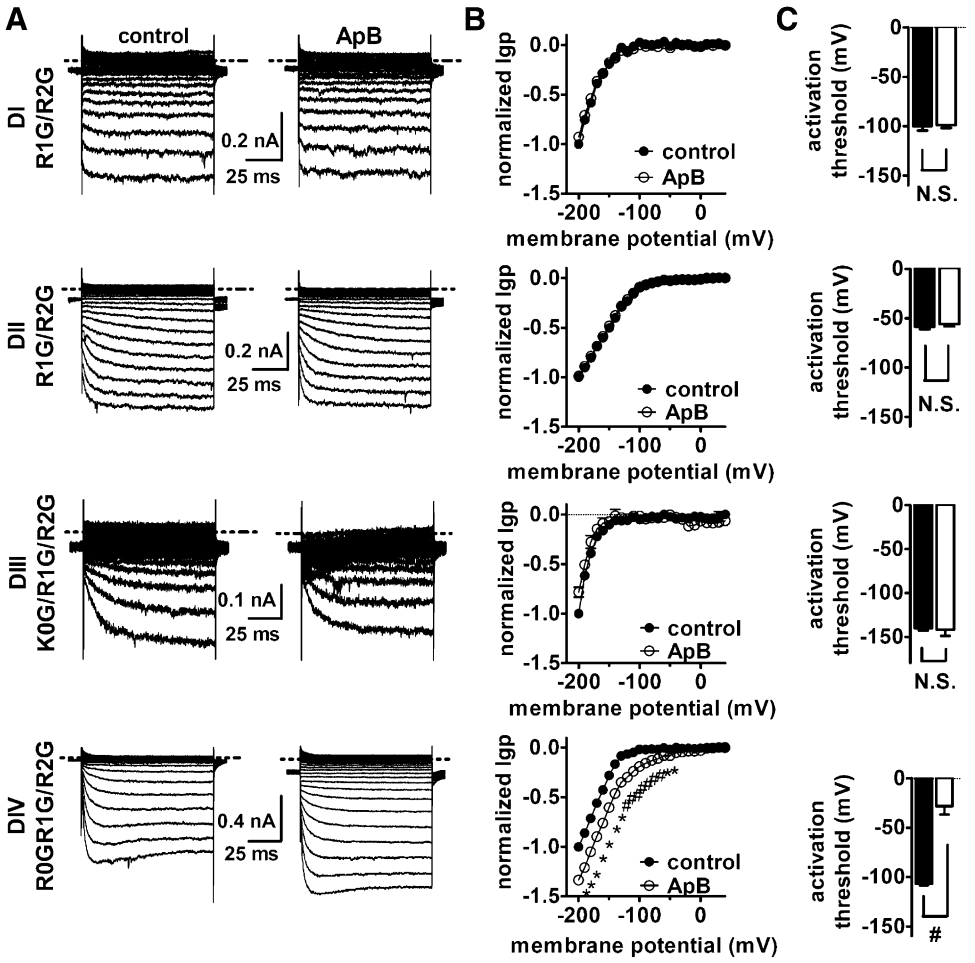


**Fig. 5.** Effect of ApB on inward Igp generated by DI–DIV voltage-sensor mutants. (A) Typical inward $hNa_v$ 1.5 Igp current traces before and after 100 nM ApB treatment. Cells were held at –100 mV and pretreated with 1 $\mu$M TTX. Currents before (left) and after (right) toxin treatment were elicited by the protocol as described in the Fig. 3 legend. The dotted line across current traces represents the zero current level. No linear leak and capacitance currents were subtracted. (B) Effect of ApB on the I–V curves of inward Igp. In all I–V curves, the subtraction of linear leak currents has been performed before (filled circles) and after (open circles) application of 100 nM ApB. Igp were normalized to the maximal control Igp. (C) Effect of ApB on the activation threshold of Igp fluxing through four voltage-sensors, respectively. N.S., no significance; $^{*}P < 0.05$; $^{\#}P < 0.01$.

of the four voltage-sensors. Our data show that 1) inward gating-pore currents, which reflect the resting configuration, can be recorded in HEK293 cells from each of the four voltage-sensors, 2) peptide toxins have unique signatures reflecting their interactions with the voltage-sensors, 3) the activity of the individual voltage-sensors are independent, and 4) the DIV voltage-sensor plays a specialized role in channel activity. Overall these data demonstrate that gating-pore currents can be used to identify molecular determinants of sodium channel gating and pharmacology.

Although gating-pore currents have previously been recorded from ion channels expressed in *Xenopus* oocytes, demonstration of gating-pore current recordings from mammalian cell lines has been lacking. Here we demonstrated that inward gating-pore currents can be recorded from each of the four voltage-sensors following sodium channel expression in HEK293 cells. Outward gating-pore currents could be recorded from DI and DII voltage-sensors. Although the gating-pore currents are smaller in mammalian cell lines and thus more challenging to record, heterologous expression of sodium channels in mammalian cell lines can have advantages. Posttranslational modifications are more probably conserved, and therefore gating and pharmacological properties should better replicate those of sodium channels in primary cells. In addition, mammalian cell lines such as HEK293 cells are more amenable to screening assays. Because gating-pore currents provide a more direct measurement of the conformation changes that individual voltage-sensors undergo, and because they have the potential to substantially alter resting membrane potential and proton flux (Wu et al., 2011), gating-pore current constructs may eventually be useful in high-throughput fluorescent screening assays for gating modifiers. However, one caveat of the approach is that it requires mutating charged residues in the S4 segments. Although mutating the outer S4 arginine residues in DII did not significantly alter sodium channel inhibition by HWTX-IV (Xiao et al., 2011) or ProTx-II (Sokolov et al., 2008a), arginine mutations can impact some toxin channel interactions (Bosmans et al., 2008) and this potential influence needs to be considered.

Our data showed that HWTX-IV selectively enhanced inward gating-pore currents generated in the DII voltage-sensor. This is consistent with HWTX-IV selectively trapping the DII voltage-sensor in the closed configuration. Although HWTX-IV can fully inhibit central-pore currents, it is interesting to note that HWTX-IV had no effect on the amplitude or voltage-dependence of gating-pore currents generated in the other three voltage-sensors. Thus trapping the DII voltage-sensor in the closed configuration is sufficient to prevent activation. Interestingly, HWTX-IV did not simply shift the voltage-dependence of the DII gating-pore currents but also seemingly enhanced the amplitude at negative potentials. This suggests that even at –200 mV, the voltage-sensor in the absence of toxin is not fully locked in the closed

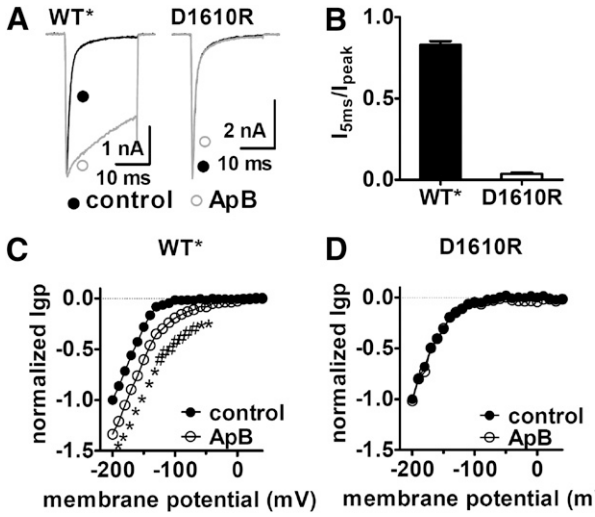


**Fig. 6.** The D1610R mutation significantly reduced the sensitivity of $Na_v$ 1.5 to ApB. (A) The D1610R mutation decreased the ability of ApB to slow fast-inactivation of $Na_v$ 1.5. Current traces before (black lines) and after (gray lines) application of 100 nM ApB were induced by a 20-ms depolarizing potential of –10 mV from a holding potential of –100 mV. (B) The ratio of $I_{5ms}$ to peak current in the presence of 100 nM ApB. $I_{5ms}$ was shown as the current not inactivated at 5 ms in (A). (C) ApB positively shifted the I–V curve of Igp fluxing through $hNa_v$ 1.5 DIV voltage-sensor mutant. (D) Single mutation D1610R abolished ApB sensitivity of DIV inward Igp. In both (C) and (D), Igp were elicited by the protocol as described in the legend of Supplemental Fig. 3. The subtraction of linear leak currents has been performed. Cells were held at –100 mV and pretreated with 1 $\mu$M TTX. All currents are normalized to the maximal control current amplitude. ApB concentration is 100 nM. Note that WT* means the triple C373Y/R800D/S802E mutant $Na_v$ 1.5 channel.

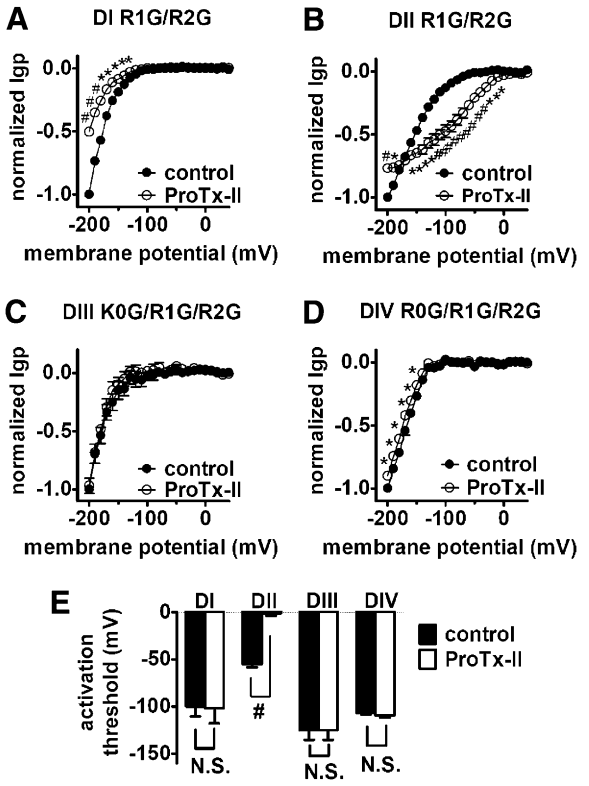


**Fig. 7.** Effect of ProTx-II on inward Igp generated by DI–DIV voltage-sensor mutants. Cells were held at –100 mV and pretreated with 1 $\mu$M TTX. Currents before (left) and after (right) 1 $\mu$M ProTx-II treatment were elicited by 100-ms hyperpolarizing steps to various potentials that ranged from –200 mV to +40 mV in a 10-mV increment. (A–D) Effects of ProTx-II on the I–V curves of inward Igp for the DI–DIV voltage-sensors, respectively. In all I–V curves, the subtraction of linear leak currents has been performed before (filled circles) and after (open circles) application of 1 $\mu$M ProTx-II. Igp were normalized to the maximal control Igp. (E) Effect of ProTx-II on the activation threshold of Igp fluxing through four voltage-sensors, respectively. N.S., no significance; $^{*}P < 0.05$; $^{\#}P < 0.01$.

position but fluctuates between configurations that do and do not allow the flow of gating-pore currents. One possibility is that HWTX-IV enhances gating-pore current amplitude by stabilizing the voltage-sensor in a position that permits a more consistent flow of ions through the gating pore. Alternative explanations include the possibility that the toxin binding alters the size of the gating pore, thus enhancing ion flow. It is difficult to determine the precise mechanism underlying the increased gating-pore current amplitude on the basis of our data presented here.

ApB selectively enhanced inward gating-pore currents generated in the DIV voltage-sensor. This is consistent with ApB selectively trapping the DIV voltage-sensor in the closed configuration. However, ApB does not inhibit central-pore currents but rather selectively impairs open channel inactivation. Thus, selectively trapping the DIV voltage-sensor in the closed configuration does not prevent the other voltage-sensors from shifting to the outward, activated configuration and inducing opening of the channel pore. Taken together these data demonstrate that the activity of the four voltage-sensors is essentially independent and that whereas activation of the DII voltage-sensor is crucial for opening the sodium channel central pore, activation of the DIV voltage-sensor is not necessary. This demonstration that the DIV voltage-sensor plays a crucial and selective role in open-channel inactivation is at odds with the proposal that inactivation does not have inherent voltage-dependence (Aldrich et al., 1983; Bezanilla and Armstrong, 1977), but consistent with more recent studies suggesting the DIV voltage-sensor has a unique specialized role in inactivation (Chen et al., 1996; Sheets et al., 1999; Yang and Kuo, 2003; Capes et al., 2013).

ProTx-II has complex actions on VGSC currents (Edgerton et al., 2008) and the molecular determinants of these actions have been elusive and controversial (Bosmans et al., 2006, 2008; Smith et al., 2007; Schmalhofer et al., 2008; Sokolov et al., 2008a; Xiao et al., 2010). Our data show that ProTx-II substantially modulates the conformation of both the DI and DII voltage-sensors in $Na_v$ 1.5. Although ProTx-II predominantly enhanced inward gating-pore currents generated in DII, indicating that it favors the resting configuration of this voltage-sensor, it inhibited inward gating-pore currents generated in DI, suggesting that it stabilizes the DI voltage-sensors into an intermediate configuration. ProTx-II is considered highly lipophilic and probably inserts into the membrane to interact with VGSCs (Smith et al., 2005). It is interesting to note that binding studies suggest that there may only be one high-affinity ProTx-II binding site on $Na_v$ 1.7 channels (Schmalhofer et al., 2008). These observations raise the intriguing possibility that a single ProTx-II molecule might simultaneously interact with the DI and DII voltage-sensors in a novel manner compared with that of other VGSC gating modifiers. Although the tarantula toxins HWTX-IV

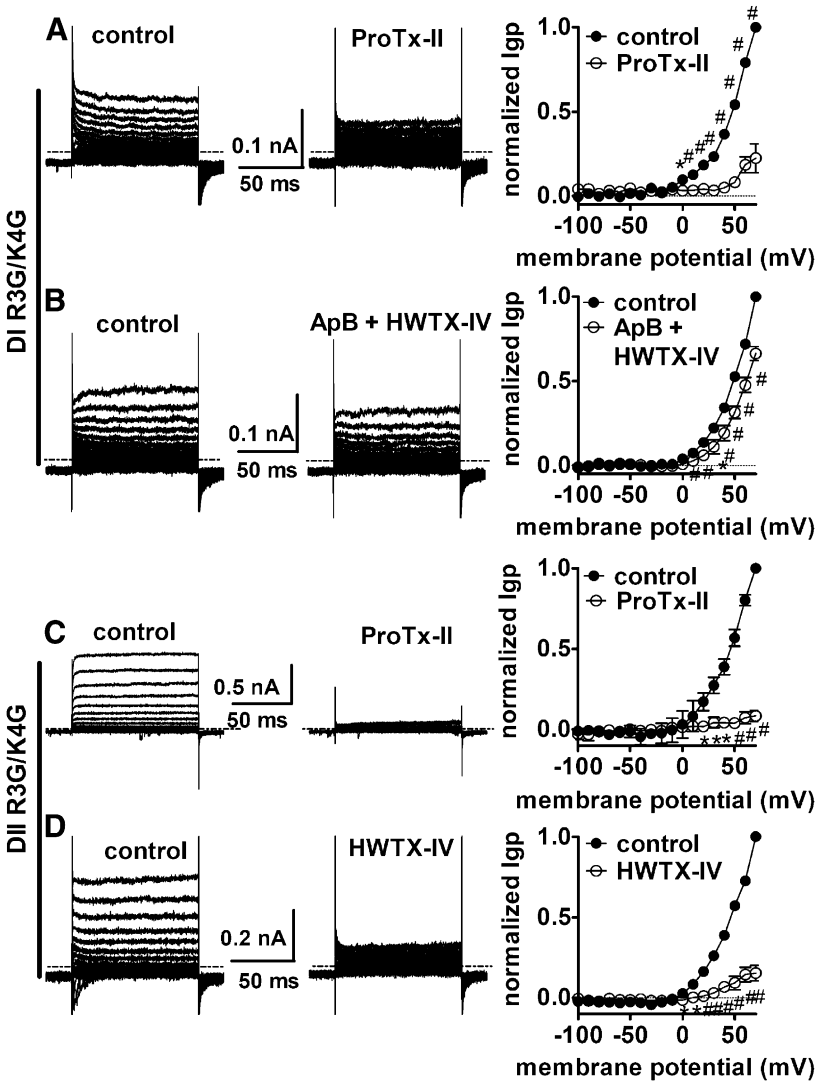


**Fig. 8.** Effects of toxins on outward Igp fluxing through $Na_v$ 1.5. Typical outward Igp current traces and associated I–V curves before and after toxin treatment are shown. (A) Effect of ProTx-II on DI outward Igp. (B) Effect of the mixture of ApB (100 nM) and HWTX-IV (1 $\mu$M) on DI outward Igp. (C) Effect of ProTx-II on DII outward Igp. (D) Effect of HWTX-IV on DII outward Igp. All currents before (left) and after (right) toxin treatment were elicited by 100-ms depolarizing steps to various potentials that ranged from –100 to +70 mV. No subtraction of linear leak and capacitance currents was performed for current traces. The dotted line across current traces represents the zero current level. Cells were pretreated with 1 $\mu$M TTX to completely block the central-pore current and held at –100 mV. Note that in the I–V curves, linear leak currents have been subtracted. $^{*}P < 0.05$; $^{\#} < 0.01$.

and ProTx-II can both inhibit sodium channel central-pore currents and interact with the DII voltage-sensor, our gating-pore current data, in conjunction with mutagenesis studies (Bosmans et al., 2008; Schmalhofer et al., 2008; Xiao et al., 2008; Xiao et al., 2010), indicate that these two peptide toxins have distinct interactions with voltage-gated sodium channels.

Overall, our data demonstrate that gating-pore currents can provide unique insight into the ability of toxins to impact the activity of individual voltage-sensors and help identify the molecular determinants of toxin-channel interactions. The gating-pore current analysis approach that we developed could also be used to explore the mechanism of action of small molecules that target voltage-gated sodium channels. Furthermore, we expect that gating-pore currents could be used to investigate of the molecular pharmacology of other voltage-gated ion channels [e.g., transient receptor potential (TRP) channels, calcium channels, potassium channels] as well.

#### Authorship Contributions

*Participated in research design:* Xiao, Blumenthal, Cummins.
*Conducted experiments:* Xiao.
*Contributed new reagents or analytic tools:* Xiao.
*Performed data analysis:* Xiao, Cummins.
*Wrote or contributed to the writing of the manuscript:* Xiao, Blumenthal, Cummins.

#### References

Aldrich RW, Corey DP, and Stevens CF (1983) A reinterpretation of mammalian sodium channel gating based on single channel recording. *Nature* **306**:436–441.
Benzinger GR, Kyle JW, Blumenthal KM, and Hanck DA (1998) A specific interaction between the cardiac sodium channel and site-3 toxin anthopleurin B. *J Biol Chem* **273**:80–84.
Bezanilla F (2008) How membrane proteins sense voltage. *Nat Rev Mol Cell Biol* **9**: 323–332.
Bezanilla F and Armstrong CM (1977) Inactivation of the sodium channel. I. Sodium current experiments. *J Gen Physiol* **70**:549–566.
Blumenthal KM and Seibert AL (2003) Voltage-gated sodium channel toxins: poisons, probes, and future promise. *Cell Biochem Biophys* **38**:215–238.
Bosmans F, Martin-Eauclaire MF, and Swartz KJ (2008) Deconstructing voltage sensor function and pharmacology in sodium channels. *Nature* **456**:202–208.
Bosmans F, Rash L, Zhu S, Diochot S, Lazdunski M, Escoubas P, and Tytgat J (2006) Four novel tarantula toxins as selective modulators of voltage-gated sodium channel subtypes. *Mol Pharmacol* **69**:419–429.
Capes DL, Arcisio-Miranda M, Jarecki BW, French RJ, and Chanda B (2012) Gating transitions in the selectivity filter region of a sodium channel are coupled to the domain IV voltage sensor. *Proc Natl Acad Sci USA* **109**:2648–2653.
Capes DL, Goldschen-Ohm MP, Arcisio-Miranda M, Bezanilla F, and Chanda B (2013) Domain IV voltage-sensor movement is both sufficient and rate limiting for fast inactivation in sodium channels. *J Gen Physiol* **142**:101–112.
Catterall WA (2002) Molecular mechanisms of gating and drug block of sodium channels. *Novartis Found Symp* **241**:206–218, discussion 218–232.
Cestèle S and Catterall WA (2000) Molecular mechanisms of neurotoxin action on voltage-gated sodium channels. *Biochimie* **82**:883–892.

Chen LQ, Santarelli V, Horn R, and Kallen RG (1996) A unique role for the S4 segment of domain 4 in the inactivation of sodium channels. *J Gen Physiol* **108**: 549–556.

Edgerton GB, Blumenthal KM, and Hanck DA (2008) Evidence for multiple effects of ProTxII on activation gating in Na(V)1.5. *Toxicon* **52**:489–500.

Gallagher MJ and Blumenthal KM (1992) Cloning and expression of wild-type and mutant forms of the cardiotonic polypeptide anthopleurin B. *J Biol Chem* **267**: 13958–13963.

George AL, Jr (2005) Inherited disorders of voltage-gated sodium channels. *J Clin Invest* **115**:1990–1999.

Lossin C, Wang DW, Rhodes TH, Vanoye CG, and George AL, Jr (2002) Molecular basis of an inherited epilepsy. *Neuron* **34**:877–884.

Middleton RE, Warren VA, Kraus RL, Hwang JC, Liu CJ, Dai G, Brochu RM, Kohler MG, Gao YD, and Garsky VM et al. (2002) Two tarantula peptides inhibit activation of multiple sodium channels. *Biochemistry* **41**:14734–14747.

Satin J, Kyle JW, Chen M, Bell P, Cribbs LL, Fozzard HA, and Rogart RB (1992) A mutant of TTX-resistant cardiac sodium channels with TTX-sensitive properties. *Science* **256**:1202–1205.

Schmalhofer WA, Calhoun J, Burrows R, Bailey T, Kohler MG, Weinglass AB, Kaczorowski GJ, Garcia ML, Koltzenburg M, and Priest BT (2008) ProTx-II, a selective inhibitor of NaV1.7 sodium channels, blocks action potential propagation in nociceptors. *Mol Pharmacol* **74**:1476–1484.

Sheets MF, Kyle JW, Kallen RG, and Hanck DA (1999) The Na channel voltage sensor associated with inactivation is localized to the external charged residues of domain IV, S4. *Biophys J* **77**:747–757.

Smith JJ, Alphy S, Seibert AL, and Blumenthal KM (2005) Differential phospholipid binding by site 3 and site 4 toxins. Implications for structural variability between voltage-sensitive sodium channel domains. *J Biol Chem* **280**:11127–11133.

Smith JJ, Cummins TR, Alphy S, and Blumenthal KM (2007) Molecular interactions of the gating modifier toxin ProTx-II with NaV 1.5: implied existence of a novel toxin binding site coupled to activation. *J Biol Chem* **282**:12687–12697.

Sokolov S, Kraus RL, Scheuer T, and Catterall WA (2008a) Inhibition of sodium channel gating by trapping the domain II voltage sensor with protoxin II. *Mol Pharmacol* **73**:1020–1028.

Sokolov S, Scheuer T, and Catterall WA (2005) Ion permeation through a voltage-sensitive gating pore in brain sodium channels having voltage sensor mutations. *Neuron* **47**:183–189.

Sokolov S, Scheuer T, and Catterall WA (2007) Gating pore current in an inherited ion channelopathy. *Nature* **446**:76–78.

Sokolov S, Scheuer T, and Catterall WA (2008b) Depolarization-activated gating pore current conducted by mutant sodium channels in potassium-sensitive normokalemic periodic paralysis. *Proc Natl Acad Sci USA* **105**:19980–19985.

Sokolov S, Scheuer T, and Catterall WA (2010) Ion permeation and block of the gating pore in the voltage sensor of NaV1.4 channels with hypokalemic periodic paralysis mutations. *J Gen Physiol* **136**:225–236.

Starace DM and Bezanilla F (2004) A proton pore in a potassium channel voltage sensor reveals a focused electric field. *Nature* **427**:548–553.

Struyk AF and Cannon SC (2007) A Na+ channel mutation linked to hypokalemic periodic paralysis exposes a proton-selective gating pore. *J Gen Physiol* **130**:11–20.

Tombola F, Pathak MM, Gorostiza P, and Isacoff EY (2007) The twisted ion-permeation pathway of a resting voltage-sensing domain. *Nature* **445**:546–549.

Tombola F, Pathak MM, and Isacoff EY (2005) Voltage-sensing arginines in a potassium channel permeate and occlude cation-selective pores. *Neuron* **45**:379–388.

Waxman SG, Dib-Hajj S, Cummins TR, and Black JA (2000) Sodium channels and their genes: dynamic expression in the normal nervous system, dysregulation in disease states(1). *Brain Res* **886**:5–14.

Wu F, Mi W, Burns DK, Fu Y, Gray HF, Struyk AF, and Cannon SC (2011) A sodium channel knockin mutant (NaV1.4-R669H) mouse model of hypokalemic periodic paralysis. *J Clin Invest* **121**:4082–4094.

Xiao Y, Bingham JP, Zhu W, Moczydlowski E, Liang S, and Cummins TR (2008) Tarantula huwentoxin-IV inhibits neuronal sodium channels by binding to receptor site 4 and trapping the domain ii voltage sensor in the closed configuration. *J Biol Chem* **283**:27300–27313.

Xiao Y, Blumenthal K, Jackson JO, 2nd, Liang S, and Cummins TR (2010) The tarantula toxins ProTx-II and huwentoxin-IV differentially interact with human Nav1.7 voltage sensors to inhibit channel activation and inactivation. *Mol Pharmacol* **78**:1124–1134.

Xiao Y, Jackson JO, 2nd, Liang S, and Cummins TR (2011) Common molecular determinants of tarantula huwentoxin-IV inhibition of Na+ channel voltage sensors in domains II and IV. *J Biol Chem* **286**:27301–27310.

Yang YC and Kuo CC (2003) The position of the fourth segment of domain 4 determines status of the inactivation gate in Na+ channels. *J Neurosci* **23**:4922–4930.

**Address correspondence to:** Dr. Theodore R. Cummins, Department of Pharmacology and Toxicology, Stark Neurosciences Research Institute, Indiana University School of Medicine, Indianapolis, IN 46202. E-mail: trcummin@iu.edu.